Chapter 15

Astronomy: A Physical Perspective
Marc L. Kutner
2009

A LOT OF MATH...
BUT GOOD EXPLANATIONS
OF STAR FORMATION

Star formation

In Chapter 14, we discussed the contents of the interstellar medium, the material out of which new stars must be formed. In this chapter, we will identify those parts of the interstellar medium that are involved in star formation, and see what we know, and what we have to learn, about the star formation process.

15.1 Gravitational binding

In Chapter 13, we talked about gravitational binding for clusters of stars. The same concepts apply to interstellar clouds, with the stars in the cluster being replaced by the particles that make up the cloud (either H or H_2). The gravitational potential energy is now due to the interaction among all of the particles in a cloud. For a uniform spherical cloud, the gravitational potential energy is $-(3/5)GM^2/R$. The kinetic energy is still related to the rms velocity dispersion, but with a large number of particles, which can easily be related to the cloud temperature, so the kinetic energy is $(3/2)(M/m)kT$, where M is the total mass of the cloud and m is the mass per particle.

The clouds are kept together by the gravitational attraction amongst all of the particles in the cloud. If the gravitational forces that hold the cloud together are greater than the forces driving it apart, we say the cloud is gravitationally bound. We can think of the random thermal motions in the gas as resisting the collapse.

The condition for gravitational binding (total energy negative) is then

$$(3/5)GM^2/R \geq (3/2)(M/m)kT$$

Dividing both sides by GM and multiplying by $(5/3)$ gives

$$(M/R) \geq (5/2)(kT/Gm) \tag{15.1}$$

The mass and radius of a cloud are not independent, since they are related to the density $\rho = M/(4\pi/3)R^3$. We might therefore like to use equation (15.1) to estimate the *smallest size cloud* of a given ρ, m and T for which the cloud is gravitationally bound. This quantity is called the *Jeans length*, R_J. *James Jeans* obtained essentially the same result with a more sophisticated analysis. We therefore eliminate M in equation (15.1), and change the inequality to an equality, since we are looking for the value of R that is on the boundary between bound and unbound. This gives

$$(4\pi/3)R_J^3\rho/R_J = 5kT/2Gm$$

Solving for R_J,

$$R_J = (15kT/8\pi Gm\rho)^{1/2} \tag{15.2}$$

Note that $(15/8\pi)^{1/2} = 0.77$, which is close to unity. As the geometry of the cloud changes, the exact value of the constant will change, but it will still be close to unity. We then write

$$R_J \cong (kT/Gm\rho)^{1/2} \tag{15.3}$$

We can rewrite this in terms of n, the number of particles per unit volume ($n = \rho/m$), as

$$R_J \cong (kT/Gm^2n)^{1/2} \tag{15.4}$$

We can also use equation (15.1) to give us the minimum mass for which a cloud of given ρ, T and m will be bound. This minimum mass is called the *Jeans mass*. It is the mass of an object whose radius is R_J, so

$$\begin{aligned} M_J &= (4\pi/3)R_J^3\rho \\ &= (4\pi/3)(kT/Gm\rho)^{3/2}\rho \\ &\cong 4(kT/Gm)^{3/2}\,\rho^{-1/2} \\ &= 4(kT/Gm)^{3/2}(nm)^{-1/2} \end{aligned} \tag{15.5}$$

Example 15.1 Jeans length and mass

Find the Jeans length and mass in a cloud with 10^5 H atoms per centimeter cubed and a temperature of 50 K.

SOLUTION

We use equation (15.4) to find R_J:

$$\begin{aligned} R_J &= \left[\frac{(1.38\times10^{-16}\,\text{erg/K})(50\,\text{K})}{(6.67\times10^{-8}\,\text{dyn cm}^2/\text{g}^2)(1.67\times10^{-24}\,\text{g})^2(10^5\,\text{cm})}\right]^{1/2} \\ &= 6.1\times10^{17}\,\text{cm} \\ &= 0.2\,\text{pc} \end{aligned}$$

We find the mass by multiplying the density by the volume:

$$\begin{aligned} M_J &= (4\pi/3)(1.67\times10^{-24}\,\text{g})(10^5\,\text{cm}^{-3})(6.1\times10^{17}\,\text{cm})^3 \\ &= 1.5\times10^{35}\,\text{g} \\ &= 76\,M_\odot \end{aligned}$$

We could have obtained the same mass directly from equation (15.5).

As we will see below, not all the mass will end up in the star.

Once a cloud becomes gravitationally bound, it will begin to collapse. We would like to be able to estimate the time for the collapse to take place. We begin by considering a particle a distance r from the center of the cloud. It will accelerate toward the center under the influence of the mass closer to the center than r. The acceleration is given by

$$\begin{aligned} a(r) &= GM(r)/r^2 \\ &= G(4\pi/3)r^3\rho/r^2 \\ &= (4\pi/3)Gr\rho \end{aligned} \tag{15.6}$$

If the acceleration of this particle stayed constant with time, then the *free-fall time*, the time for it to fall a distance r, would be

$$\begin{aligned} t_{ff} &= \left[\frac{2r}{a(r)}\right]^{1/2} \\ &= \left[\frac{2r}{(4\pi/3)(Gr\rho)}\right]^{1/2} \end{aligned} \tag{15.7}$$

Note that the constant $(3/2\pi)^{1/2} = 0.7$, which we can approximate as unity, since we are making an estimate of the time. This gives

$$t_{ff} \cong 1/(G\rho)^{1/2} \tag{15.8}$$

The free-fall time is independent of the starting radius. Therefore, all matter in a constant density cloud has approximately the same free-fall time. However, as the cloud collapses, the density increases. The collapse proceeds faster. The free-fall time for the original cloud is therefore an upper limit to the actual collapse time. However, the result is not very different, since most of the time will be taken up in the early stages of the collapse, when the acceleration is not appreciably different from the one we have calculated. Therefore, we use the free-fall time as a reasonable estimate of the time it will take a cloud to collapse.

There is one important difference between our idealized cloud and a real cloud. A real cloud will probably have a higher density in the center. We can see this as follows. If the cloud is initially of uniform density, all points will have the same inward acceleration. This means that all particles will cover the same inward distance dr (where $dr < 0$), in some time interval dt. We can see how this changes the density for different volume spheres. If the initial density is ρ_0, then the density of a constant mass collapsing sphere that shrinks from r_0 to r is

$$\rho = \rho_0\,(r_0/r)^3$$

The change in density $d\rho$ is found by differentiating to give

$$d\rho = -3\,\rho_0\,(r_0^3/r^4)\,dr$$

The fractional change in density, $d\rho/\rho$, is

$$d\rho/\rho = -3\, dr/r \tag{15.9}$$

This means that the smaller the initial sphere we consider, the faster its density will grow.

With a higher density at the center, the free-fall time for material near the center will be less than for material near the edge. The material from the edge will lag behind the material closer in. This will enhance the density concentration in the center. The net result is that we end up with a strong concentration in the center. The concentration will eventually become the star, but the material from the outer parts of the cloud will continue to fall in on the star for quite some time.

Example 15.2 Free-fall time

Calculate the free-fall time for the cloud in the above example.

SOLUTION

Using equation (15.8) gives

$$t_{ff} = [(6.67 \times 10^{-8}\ \text{dyn cm}^2/\text{g}^2)(1.67 \times 10^{-24}\ \text{g})(10^5\ \text{cm}^{-3})]^{-1/2}$$

$$= 9.5 \times 10^{12}\ \text{s}$$

$$= 3 \times 10^5\ \text{yr}$$

While almost a million years might sound like a long time, it is short compared with the main sequence lifetime of the star that will be formed, or the age of the galaxy.

If the cloud is rotating, then the collapse will be affected by the fact that the cloud's angular momentum must remain constant. The angular momentum L is the product of the moment of inertia I and the angular speed ω,

$$L = I\,\omega \tag{15.10}$$

For a uniform sphere, the moment of inertia is

$$I = (2/5)Mr^2 \tag{15.11}$$

If I_0 and ω_0 are the original moment of inertia and angular speed, and I and ω are their values at some later time, conservation of angular momentum tells us that

$$I_0\,\omega_0 = I\,\omega \tag{15.12}$$

Using equation (15.11) to eliminate I and I_0, we have

$$(\omega/\omega_0) = (r_0/r)^2 \tag{15.13}$$

(This explains why a figure skater rotates faster as she brings her arms in. The $1/r^2$ dependence of the angular speed has a dramatic effect.)

To see what effect this has on collapse, we again look at a particle a distance r from the center of a collapsing cloud. The acceleration at that point is still $GM(r)/r^2$. However, the radial acceleration now has two parts: (1) $a(r)$ is associated with the change in magnitude of the radius, and (2) the acceleration associated with the change of direction, $r\omega^2$. Therefore,

$$GM(r)/r^2 = a(r) + r\omega^2 \tag{15.14a}$$

Solving for $a(r)$ gives

$$a(r) = GM(r)/r^2 - r\omega^2 \tag{15.14b}$$

In comparing this with equation (15.6), we see that the acceleration $a(r)$ is less for a rotating cloud than for a non-rotating cloud. The effect of the rotation is to slow down the collapse perpendicular to the axis of rotation.

The effects of rotation will be most significant when the second term on the right-hand side of equation (15.14a) is much greater than the first term, in which case

$$GM(r)/r^2 = r\omega^2$$

Multiplying both sides by r^2 gives

$$GM(r) = r^3\omega^2$$

$$= r^3\omega_0^2\,(r_0/r)^4$$

$$= (\omega_0 r_0)^2\,(r_0/r)\,r_0 \tag{15.15}$$

Noting that $v_0 = \omega_0\, r_0$, where v_0 is the speed of a particle a distance r_0 from the center,

$$GM(r) = v_0^2\, r_0\, (r_0/r)$$

We now solve for r/r_0, the amount by which the cloud collapses before the rotation dominates:

$$r/r_0 = v_0^2\, r_0/\, GM(r) \tag{15.16}$$

For the cloud given in the two previous examples, with an initial rotation speed $v_0 = 1$ km/s, $r/r_0 = 0.6$. This means that, by the time the cloud

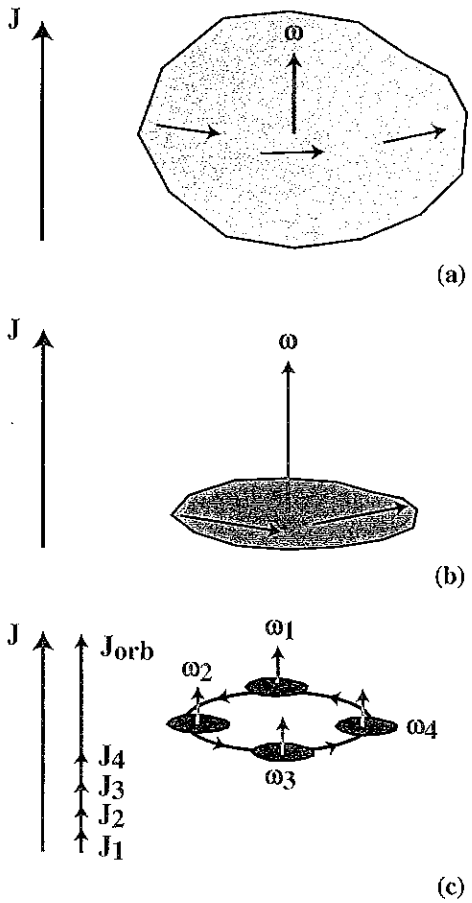

Fig. 15.1 Fragmentation of a collapsing interstellar cloud. (a) The cloud is initially rotating as shown. As it collapses, the angular momentum **J** is conserved. (b) As the cloud becomes smaller, its angular speed ω must increase to keep the angular momentum fixed. The rotation inhibits collapse perpendicular to the axis of rotation, and the cloud flattens. (c) Unable to collapse any further, the cloud breaks up, with the total angular momentum being divided between the spin and orbital angular momenta of the individual fragments.

reaches half its initial size, the rotation can completely stop the collapse perpendicular to the axis of rotation. Motions parallel to the axis of rotation are not affected by this, so collapse parallel to the axis of rotation can proceed unimpeded, and the cloud will flatten. (We will see that the tendency of rotating objects to form disks will reappear in many astrophysical situations.) Since the collapse is then only in one dimension, it is harder to reach stellar densities. Thus, the effect of rotation is to keep much of the material from becoming a star.

More of the material can end up in stars if the cloud breaks up into a multiple star system. The angular momentum can be taken up in the orbital motion, but individual clumps can continue contracting. This fragmentation process is probably responsible for the high incidence of binary systems. If a cloud shrinks to half its initial size, the average density will go up by a factor of eight. (The density is proportional to 1/volume, and the volume is proportional to r^3.) From equation (15.5), we see that the Jeans mass of the denser cloud will be approximately one-third of the original Jeans mass. This means that it is possible for the less massive clumps to be bound and continue their collapse. The fragmentation process (Fig. 15.1) may be repeated until stellar mass objects are reached.

15.2 | Problems in star formation

We would like to know the conditions under which stars will form. We would like to know which types of interstellar clouds are most likely to form stars, and which locations within the clouds are the most likely sites of star formation. We would also like to know whether star formation is spontaneous or whether it needs some outside *trigger*. When we say a trigger is necessary, we mean that the conditions in a cloud are right for star formation, but something is necessary to compress the cloud somewhat to get the process started. Once started, it continues on its own. Sources for triggering star formation that have been suggested are the passage of a supernova remnant shock front, or the compression caused by a stellar wind. (Later in this chapter we will see how expanding HII regions might act as triggers, and in Chapter 17 we will discuss density waves associated with galactic spiral structure. These might also induce star formation.)

Once the collapse to form stars starts, we would like to know how it proceeds, and what fraction of the cloud mass ends up in stars. This is sometimes referred to as the *efficiency of star formation*. We would also like to know how much of the mass that goes into stars goes into stars of various masses. This is called the *initial mass function*. By "initial" we mean the distribution of stellar

masses at the time that a cloud gives birth to stars. The actual mass distribution in the galaxy is altered by the fact that stars of different masses have different lifetimes.

An important problem in understanding the evolution of star forming clouds comes from the angular momentum of the cloud. In the previous section, we saw that the collapse can be slowed down or even stopped in a rotating cloud. How a cloud distributes and loses its angular momentum probably affects the efficiency of star formation and the initial mass function. In addition, it may account for the high fraction of multiple star systems and for the formation of planetary systems.

An interesting set of problems is posed by groupings of stars called *OB associations*. These are groups of stars in which it has been suggested that all O stars form. We refer to these groupings as associations rather than clusters because associations are not gravitationally bound. They are expanding, and eventually dissolve into the background of stars. We would like to know how an initially bound cloud can give birth to an unbound grouping of stars. In Chapter 13 we saw that, if a system in virial equilibrium loses more than half of its mass without the velocity distribution changing, then the system becomes unbound. It is clear that the clusters have lost more than half their mass.

Another interesting feature of OB associations is the existence of *subgroups*. Some associations have as many as three or four distinct groupings of stars. The subgroups have different ages, as determined from their HR diagrams. Also, the older subgroups seem to be larger, which makes sense if they are expanding. A major question in star formation is explaining what appears to be a sequential wave of star formation through an association. It is in this context that triggers have been most actively discussed. OB associations are often near molecular clouds, as shown in Fig. 15.2. The younger subgroups tend to appear closer to the molecular clouds.

We would also like to know whether low and high mass star formation take place in different ways or in different environments. It has been suggested, for example, that low mass stars are being made all the time, whereas high mass star formation takes place in bursts. We would also like to know how an interstellar cloud knows what distribution of stellar masses it is supposed to make.

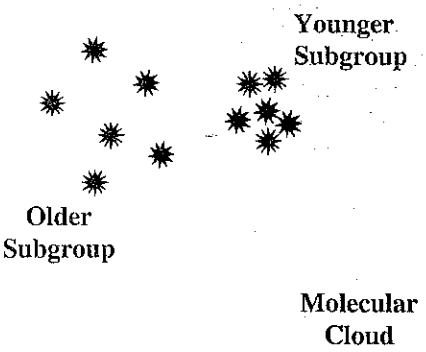

Fig. 15.2 OB associations and molecular clouds. These associations often have a few subgroups. The older subgroups are more extended, since the associations are unbound and are expanding. Younger subgroups tend to be more closely related to molecular clouds.

15.3 Molecular clouds and star formation

We discussed the properties of molecular clouds in Chapter 14. They are important for star formation because they are both cool and dense, relative to the rest of the interstellar medium. In Section 15.1, we discussed the conditions under which an interstellar cloud is gravitationally bound, and expressed the result as a Jeans length. For a cloud of a given temperature T and number density n, the Jeans length is the minimum size of a gravitationally bound cloud. We approximated the Jeans length (equation 15.4) as

$$R_J \cong (kT/Gm^2n)^{1/2}$$

Example 15.3 Jeans length for atomic and molecular clouds

Compare the Jeans length for an atomic cloud ($T = 100$ K, $n = 1$ cm^{-3}) and a molecular cloud ($T = 10$ K, $n = 10^3$ cm^{-3}).

SOLUTION

We simply take the ratios, noting also that the mass per particle in molecular clouds is twice that in atomic clouds.

$$R_J(\text{at})/R_J(\text{mol}) = [(10^3)(10)(4)]^{1/2}$$
$$= 200$$

This means that a much smaller piece of a molecular cloud can become gravitationally bound than for an atomic cloud. It is therefore much easier to get a bound section in a molecular cloud than in an HI cloud. This comes about because of both the higher density and lower temperature.

We find a number of different types of molecular clouds. Their basic properties are summarized in Table 15.1. The simplest are the globules, as shown in Fig. 14.1. These are sometimes called *Bok globules*, after *Bart Bok*, who suggested that they were potential sites for star formation. Globules are typically a few parsecs across. They generally have a simple, round appearance. This simplicity makes them attractive to study. Their visual extinctions fall in the range 1–10 mag, which can be determined by star counting. From CO observations, we find their kinetic temperatures are about 10 K. From observations of CO and CS we estimate their densities at 10^3 cm^{-3} and up to 10^4 cm^{-3}, and masses in the range 10 to 100 $M_\odot$. We think that they are in a state of slow gravitational contraction.

The *dark clouds*, such as those shown in Fig. 15.3, have local conditions (density, temperature) similar to those in globules, but the dark clouds are larger. Typical sizes for the dark clouds are in the tens of parsecs range. Often a size is hard to define because dark clouds appear to consist of a number of small clouds in an irregular arrangement. There is evidence that they contain low mass stars.

Fig. 15.3 Dark clouds blocking the light from background stars. Note the intricate shapes. This is a near infrared image of the star forming region RCW108. We see a few bright young stars, but mostly irregular dark clouds. (Compare this with the simple shape of the globule in Fig. 14.1.) [ESO]

The largest molecular clouds are called *giant molecular clouds* or *GMCs*. They are generally elongated, with a length of about 50 to 100 pc. Their

Table 15.1. | Interstellar molecular clouds.

Type	T_k (K)	$n(H_2)$ (cm^{-3})	R (pc)	M ($M_\odot$)	A_V (mag)	Probes
Dark cloud	10	10^3	5–10	10^4	1–6	CO
Globule	10	10^3–10^4	1	10^2–10^3	5–15	CO, CS
GMC envelope	15	300	50	10^5	1–5	CO
Dense core	30–100	10^5–10^6	1	10^3	100	CO, CS, H_2CO, NH_3 and many others
Protostellar cores	100–200	10^7				high j transitions of various molecules
Energetic flows	1000					CO, SiO, H_2
Envelope of evolved stars	2000					SiO masers

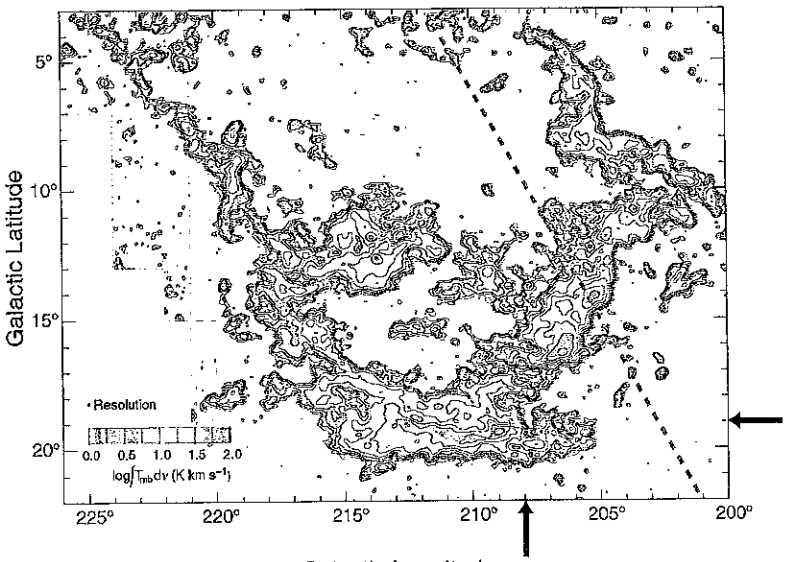

Fig. 15.1 Molecular clouds in the Orion region. Giant molecular clouds are indicated by their contours of emission from the CO molecule at 2.6 mm. This was done with a 1 m telescope, providing an angular resolution of 12 arc min, which, as the black dot at lower left shows, is quite adequate for this map. This was part of a survey of CO emission in our galaxy (which we will talk about more in the next chapter), so this is plotted in galactic coordinates, which are tilted with respect to the celestial equator, which is shown in a red dashed line in this figure. The Orion Nebula (shown in Fig. 15.28) is at the intersection of the two black arrows in the lower right corner of the figure. At the 500 pc distance of Orion, 100 pc would subtend 11 degrees. So, the cloud containing the Orion Nebula is some 80 pc long. There is an OB association around the region of the nebula. There is another equally large cloud that extends to the north across the celestial equator. This contains the association connected to Orion's belt and includes (as a very small part) the Horsehead Nebula (Fig. 14.3). Note that there are some other clouds which extend to the west, into Monoceros, containing yet another OB association. [Thomas Dame, CFA]

densities are about 300 cm^{-3}, a little lower than for globules or dark clouds. They are also warmer, with $T = 15$ K. Their extent can be traced using CO observations, like those shown in Fig. 15.4. By observing CO in nearby GMCs, where we can see the dust, we gain confidence in the fact that the CO tells us where the dust (and molecular hydrogen) is. We therefore use the CO to trace out GMCs that are so far away that foreground dust blocks our view of them. GMCs typically have masses of a few times 10^5 $M_\odot$, and seem to come in complexes whose masses exceed 10^6 $M_\odot$. These complexes are among the most massive entities in the galaxy. There seems to be a close connection between giant molecular clouds and OB associations. It therefore appears that O and B stars form in GMCs. GMCs also have lower mass stars in addition to the O and B stars.

Within the giant molecular clouds we find denser regions, called *dense cloud cores*. These are denser and warmer than the surrounding cloud. Their temperatures are above 50 K. Their densities, determined from studies of a number of different molecules, are in the range 10^5 to 10^6 cm^{-3}. (Even though we call these clouds "dense", their densities are comparable to the best vacuums we can obtain in the laboratory!) These cores are small, only a few tenths of a parsec across, and have masses of a few hundred $M_\odot$. Our ability to study them is limited by the angular resolution of our telescopes, but that is helped by the development of interferometers working at millimeter wavelengths. We think that these cores are the places in the GMCs where the star formation is taking place. (Some dense cores are also found in dark clouds and globules.)

One of the observational challenges in studying dense cloud cores is to find cores in which there is unambiguous evidence for collapse. After

all, if these are in the process of forming stars, there should be large inward motions that should be detectable via Doppler shifts. Material on the side of the core closest to us should be moving away from us, and we should see redshifted spectral lines. Material on the far side of the core should be moving towards us, and we should see blueshifted spectral lines. We do see objects with both large red- and blueshifts. The problem is that the Doppler shift measurements cannot tell us which side of the cloud each part of the emission is coming from. So, an expanding cloud could have the same spectra as a collapsing cloud. The trick lies in having high angular resolution and seeing how the Doppler shift changes with position. Studies of possible collapsing clouds using millimeter interferometers are just beginning to yield results.

In our discussions, it is important to remember that, while we think in terms of spherical clouds for simplicity, real clouds have irregular shapes. Most of the larger clouds (GMCs) appear elongated, part of larger filamentary structures. It has even been suggested that the geometry of interstellar clouds may be better represented by fractals. However, we can still form a good insight into the physical processes that govern star formation using our simplified models.

15.4 Magnetic effects and star formation

Astronomers are becoming increasingly aware of the fact that magnetic fields can have an important effect on the star formation in an interstellar cloud. Work in this area has been slow for two reasons. (1) As we have seen, measurements of the interstellar magnetic fields are very difficult. Until we have a good idea of field strengths, it is hard to estimate their effects. As we mentioned in the last chapter, observations of the Zeeman effect in HI yield field intensities of tens of microgauss in a number of clouds. (2) Theories that include magnetic fields are much harder to work out than those that don't. However, computer simulations of gravitational collapse in clouds with substantial magnetic fields are being carried out more routinely.

We would expect the magnetic effects to be important when the energy associated with the presence of the magnetic field is comparable to the gravitational energy in magnitude. In cgs units, the energy density (erg/cm^3) associated with a magnetic field B is

$$u_B = B^2/8\pi \tag{15.17}$$

Example 15.4 Magnetic energy

For what magnetic field strength B does the magnetic energy of a cloud equal the absolute value of the gravitational potential energy? Assume a spherical cloud with a radius $R = 10$ pc, and a density of molecular hydrogen $n(H_2) = 300$ cm^{-3}.

SOLUTION

The magnetic energy U_B is the energy density, multiplied by the volume of the cloud:

$$U_B = \left(\frac{B^2}{8\pi}\right)\left(\frac{4\pi}{3}\right)R^3$$

$$= \frac{B^2R^3}{6}$$

The magnitude of the (negative) gravitational potential energy is

$$-U_G = \frac{3}{5}\frac{GM^2}{R}$$

$$= \frac{3}{5}G\frac{\left[\left(\frac{4\pi}{3}R^3\right)n(H_2)(2m_p)\right]^2}{R}$$

$$= \left(\frac{16\pi^2}{15}\right)GR^5(n(H_2)(2m_p))^2$$

$$= 10\,GR^5\,(n(H_2)(2m_p))^2$$

Equating these and solving for B, we have

$$B = (60\,G)^{1/2}\,(2n(H_2)m_p\,R)$$

$$= 6 \times 10^{-5} \text{ gauss}$$

$$= 60\ \mu\text{G}$$

This is of the order of strengths of fields that have been measured from HI Zeeman measurements.

As a molecular cloud collapses, the magnetic field strength will increase, as illustrated in Fig. 15.5. This is because of the flux freezing, discussed in Chapter 11. (Remember, Faraday's law

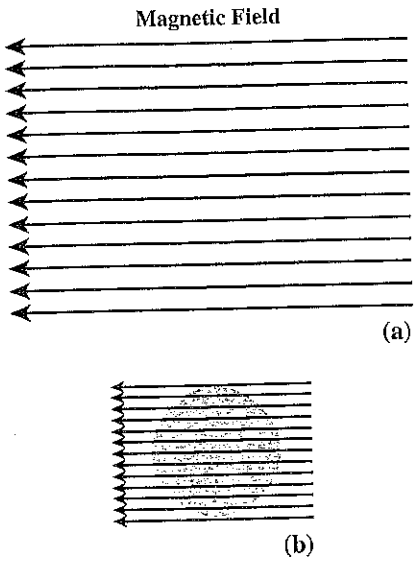

FIG 15.5 Flux freezing in a collapsing interstellar cloud. Graphically, Faraday's law tells us that the number of field lines crossing the cloud's surface stays constant as the cloud collapses. This means that the field lines are closer together, signifying a stronger field in (b).

requires that the flux through a conducting surface be constant.) This only takes place if the cloud is a good conductor. Most interstellar clouds have sufficient ionization for this to be the case. The ionization in cold clouds probably results mostly from cosmic rays. Most of the mass of the cloud is in the form of neutral atoms or molecules. There are roughly 10^7 neutrals for every ion. However, as the cloud collapses, these neutral particles carry the charged particles along with them. The charged particles, in turn, provide the conductivity to insure the flux freezing. This process allows the magnetic field effectively to exert a pressure which can inhibit the collapse.

Example 15.5 Flux freezing

For a spherical cloud with the magnetic flux constant as the cloud collapses, find how the magnetic energy varies with the cloud radius R. Compare this with the gravitational energy.

SOLUTION

For a uniform cloud, the magnetic flux is the product of the field B and the projected area of the cloud πR^2. This means that the flux is proportional to BR^2. If the flux is constant, then BR^2 must be constant. This means that

$$B \propto 1/R^2$$

From the previous example, we see that the magnetic energy U_B is proportional to B^2R^3. This means that

$$U_B \propto (1/R^2)^2 R^3$$

$$\propto 1/R$$

The gravitational potential energy is

$$U_G \propto GM^2/R$$

Since the mass of the cloud stays constant as it collapses,

$$U_G \propto 1/R$$

Therefore, the magnetic and gravitational energies have the same dependence on R as the cloud collapses. If the magnetic field cannot prevent the initial collapse, then it cannot prevent the further collapse. However, if the magnetic field is important in the initial collapse, it will continue to be important.

As a cloud evolves, the ions and neutrals do not always stay perfectly mixed. The ions drift with respect to the neutrals. If this happens, some of the magnetic flux will escape from the cloud, meaning that the field is not as high as one would calculate from flux freezing. The process, called *ambipolar diffusion*, has another effect. As the ions move past the neutrals some collisions occur. This converts some of the drift motion into random motions of the neutrals, meaning an increase in the cloud temperature. Therefore, ambipolar diffusion can serve as a general heat source in a cloud.

The current picture that has emerged suggests that there are two ways in which the magnetic support of clouds is overcome. One is by ambipolar diffusion. This occurs in clouds where the magnetic energy is comparable to the gravitational energy. Ambipolar diffusion allows for the gradual contraction of the cloud. It is thought that this process produces low mass stars at a roughly steady rate throughout the galaxy. In the alternative situation enough material is gathered together so that the absolute value of the gravitational

energy is much greater than the magnetic energy, and star formation takes place rapidly. It is thought that this process makes a mixture of high and low mass stars.

15.5 Protostars

15.5.1 Luminosity of collapsing clouds

As a cloud collapses the gravitational potential energy decreases. This is because the particles within the cloud are moving closer to the center. The decrease in potential energy must be offset by energy radiated away or by an increase in the kinetic energy. This increased kinetic energy can show up in two forms: (1) it can go into the faster infall of the particles in the collapsing cloud; or (2) it can go into heating the cloud.

Let's see what happens to the energy in a collapsing cloud. From the virial theorem, we know

$$E = -\langle K \rangle \tag{15.18}$$

This tells us that as the cloud collapses its internal kinetic energy K will increase. However, only half the potential energy shows up as increased kinetic energy. We can therefore see that the total energy of the collapsing cloud is decreasing. This means that the cloud must be radiating energy away. The virial theorem tells us that half of the lost potential energy shows up as kinetic energy, and half the energy is radiated away.

We can relate the luminosity of a contracting cloud to its total energy. The total energy is

$$E = (-3/10)GM^2/R \tag{15.19}$$

The energy lost in radiation must be balanced by a corresponding decrease in E. The luminosity, L, must therefore be equal to dE/dt. Differentiating equation (15.19) gives

$$\frac{dE}{dt} = \frac{3}{10}\left(\frac{GM^2}{R^2}\right)\left(\frac{dR}{dt}\right) \tag{15.20}$$

We can solve for dR/dt to find the collapse rate for a given luminosity:

$$\frac{dR}{dt} = \frac{10}{3}\left(\frac{R^2}{GM^2}\right)\left(\frac{dE}{dt}\right) \tag{15.21}$$

(Remember, for a collapsing cloud, both dR/dt and dE/dt are negative numbers.) If we solve equation (15.19) for R, and substitute that solution for one of the R's in equation (15.20) or (15.21), we find that

$$\frac{1}{E}\frac{dE}{dt} = \frac{1}{R}\left(\frac{dR}{dt}\right) \tag{15.22}$$

This tells us that, in any time interval dt, the fractional change in the energy dE/E is equal to the fractional change in the radius dR/R. These results tell us that the rate of collapse can be limited by the rate at which energy can be radiated.

We now look at the luminosity in various stages of the collapse. As the collapsing cloud heats, it is still well below normal stellar temperatures, so most of the radiation is given off in the infrared. Therefore, the opacity of the cloud in the infrared plays an important role in determining the nature of the collapse.

When the collapse begins, the material is mostly atomic and molecular hydrogen and atomic helium. As the collapse continues, half the liberated energy goes into the internal energy of the gas. However, this doesn't increase the temperature. Instead, the energy goes into the ionization of these neutral species. Following this, the liberated energy goes into heating the gas, and the gas pressure can eventually slow the collapse. For a 1 $M_\odot$ protostar, the free-fall phase ends when the radius is about 500 $R_\odot$. (The radius varies approximately with mass.) During the free-fall stage, the luminosity increases and $|dR/dt|$ increases.

Example 15.6 Luminosity of a collapsing cloud
For a 1 $M_\odot$ protostar that has collapsed to a radius of 500 $R_\odot$, (a) calculate the energy that has been liberated to this point; (b) use this to calculate the average luminosity if most of the energy is liberated in the last 100 years of the collapse.

SOLUTION
From the virial theorem, the energy radiated will be one-half times the current gravitational potential energy:

$$E = -\left(\frac{1}{2}\right)\left(-\frac{3}{5}\right)\frac{GM^2}{R}$$

$$= \left(\frac{3}{10}\right)\frac{(6.67 \times 10^{-8}\,\text{dyn cm}^2/\text{g}^2)(2 \times 10^{33}\,\text{g})^2}{(500)(7 \times 10^{10}\,\text{cm})}$$

$$= 2 \times 10^{45}\,\text{erg}$$

The average luminosity is this energy divided by the time over which it is radiated:

$$L(\text{avg}) = \frac{2 \times 10^{45}\,\text{erg}}{(100)(3 \times 10^{7}\,\text{s})}$$

$$= 7 \times 10^{35}\,\text{erg/s}$$

$$= 170\,L_{\odot}$$

This is the average luminosity over the 100 year period, but the actual luminosity at the end of the period is higher, since $|dR/dt|$ is greatest then.

Once a cloud is producing stellar luminosities by gravitational collapse, we call it a *protostar*. Once the cloud becomes opaque the radiation can only escape from near the surface. (When the opacity is low a photon can escape from anywhere within the volume.) Since energy escapes slowly, the temperature rises quickly. Also, a large temperature difference can exist between the center and the edge. Under these conditions, the most efficient form of energy transport from the center to just outside is by convection. This point was first realized in 1961 by the Japanese astrophysicist Chushiro Hayashi. During this stage the surface temperature stays roughly constant at about 2500 K. Since the radius is decreasing, and the temperature is approximately constant, the luminosity decreases.

During this stage the central temperature is still rising. When it is high enough, nuclear reactions start. The contraction goes on for some time in the outer parts, as the pressure builds up in the core. Eventually the pressure in the core is sufficient to halt the collapse, and the star is ready to settle into its main sequence existence.

For a protostar, the continuous spectrum peaks in the near infrared. The dust in the collapsing cloud surrounding the protostar will absorb some of the radiation. The dust will be heated, but will not be the same temperature as the star. The emission from the dust will be in the far infrared. From this we see that protostars are best observed in the infrared part of the spectrum.

15.5.2 Evolutionary tracks for protostars

When we plot an HR diagram with stars we see now, we are plotting the distribution of L and T as they are now. However, as a star evolves, its luminosity and temperature change. Therefore, its location on an HR diagram changes. If $L(t)$ is the luminosity of a star as a function of time and $T(t)$ is the temperature as a function of time, we can plot a series of points and connect them to follow the evolution of a star. Such a series of points is called an evolutionary track. Stars evolve so slowly compared with human lifetimes that we cannot deduce the evolutionary track by observing one star. However, by observing many stars, each at a different stage, we can infer the evolutionary tracks. (We have already used evolutionary tracks in our discussion of post main sequence evolution, in Chapters 10 and 11.)

We can also predict evolutionary tracks from theoretical models of protostars and stars. We use basic physics to calculate the physical conditions, and see how the star's radius and temperature change with time. Since the luminosity is given by $L = (4\pi R^2)(\sigma T^4)$, we can relate changes in R and T to changes in L and T. When we calculate model tracks, we find that the evolutionary track of a protostar depends on its mass. This is not surprising, since we have already seen that the mass determines where a star will appear on the main sequence.

Some evolutionary tracks for protostars and pre-main sequence stars are shown in Fig. 15.6. Note that the protostars appear above the main sequence. This means that for a given temperature, T, protostars are more luminous than main sequence stars of the same temperature. Protostars are also larger than main sequence stars of the same temperature. This is not surprising since protostars are still collapsing. Once the accretion phase stops, but before the main sequence is reached, we call these objects *pre-main sequence stars*.

Fig. 15.7 shows a model for the collapse of an interstellar cloud into a 1 $M_{\odot}$ protostar. At first the cloud is cool, and then it contracts and heats. As discussed above, the T^4 increase is greater than the R^2 decrease, and the luminosity of the protostar increases. The peak luminosity is reached when the temperature reaches 600 K. As the protostar becomes denser, its opacity increases. Eventually, it is harder for the radiation from the center to escape, and the luminosity begins to decrease. During this stage energy transport in

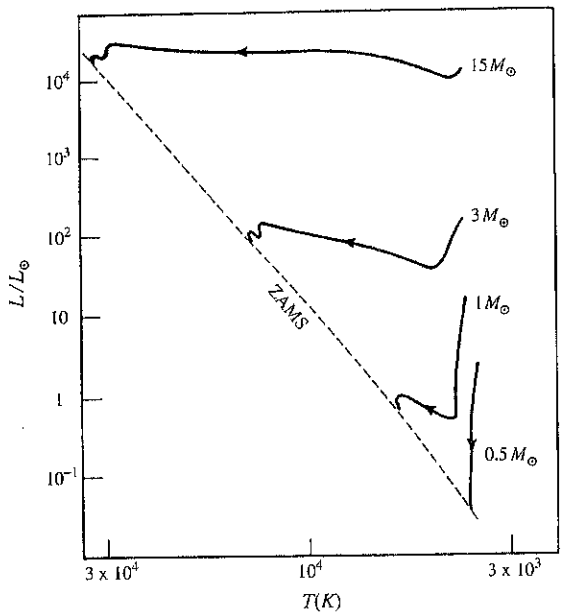

Fig. 15.6 Evolutionary tracks for pre-main sequence stars on an HR diagram. Tracks are marked by the mass used in the model. The dashed line represents the zero age main sequence (ZAMS), the place where stars first join the main sequence.

the star is mostly by convection. The part of the evolutionary track at which the luminosity is decreasing quickly while the temperature increases slightly is called the *Hayashi track*. After this collapse slows, the star begins to approach the main sequence. Eventually, it reaches the luminosity of a main sequence star, though it may vary somewhat before settling down.

15.6 Regions of recent star formation

When we study star formation, we find that there are some very obvious signposts of recent or ongoing star formation. Regions of recent star formation are important for a number of reasons. First, they call our attention to places where star formation might still be taking place. Second, the newly formed stars have some effect on their immediate vicinity, which might promote or inhibit further star formation. In this section we will look at some of the most prominent: (a) HII regions, (b) masers, (c) energetic flows, and (d) protostellar cores. In each case the object becomes prominent either because of the unique conditions that accompany star formation or because of the effect of newly formed stars on the cloud out of which they were born.

15.6.1 HII regions

When a massive star forms it gives off visible and ultraviolet photons. Photons with wavelengths shorter than 91.2 nm, in the ultraviolet, have enough energy (> 13.6 eV) to ionize H. The stars that give off sufficient ultraviolet radiation to cause significant ionization are the O and early B stars. When most of the hydrogen is ionized, we call the resulting part of the cloud an *HII region*, as shown in Fig. 15.8.

In equilibrium in an HII region there is a balance between ionizations and recombinations.

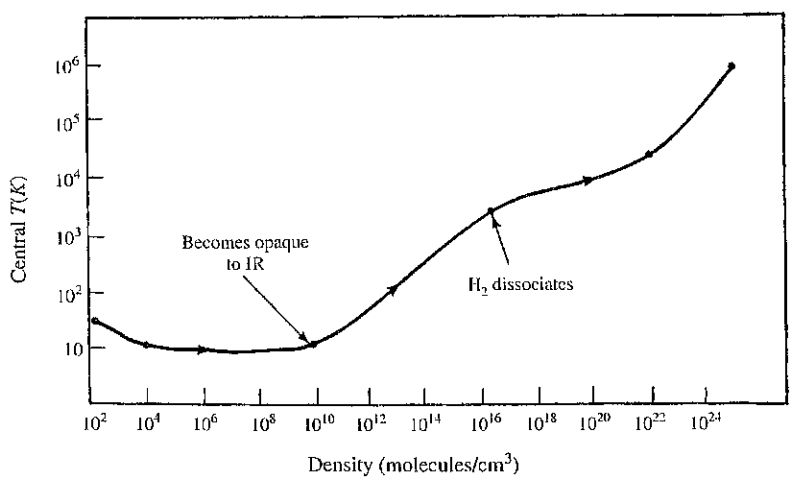

Fig. 15.7 Model for the collapse of an interstellar cloud into a protostar and a pre-main sequence star.

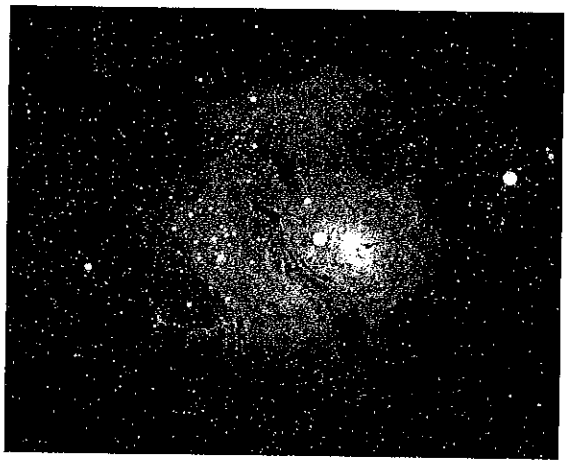

(a)

(d)

(b)

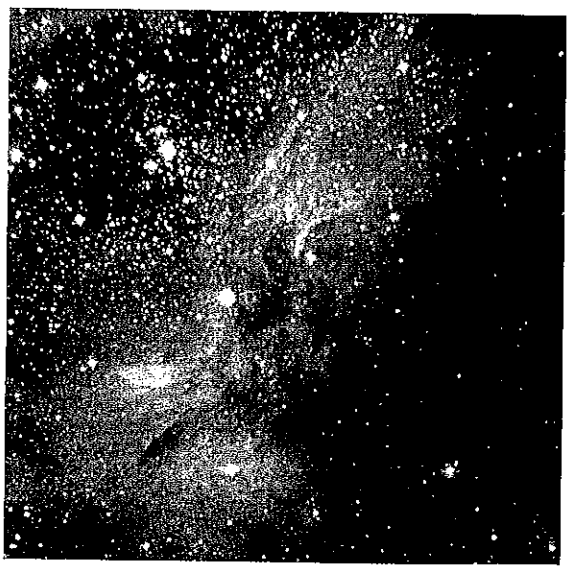

(e)

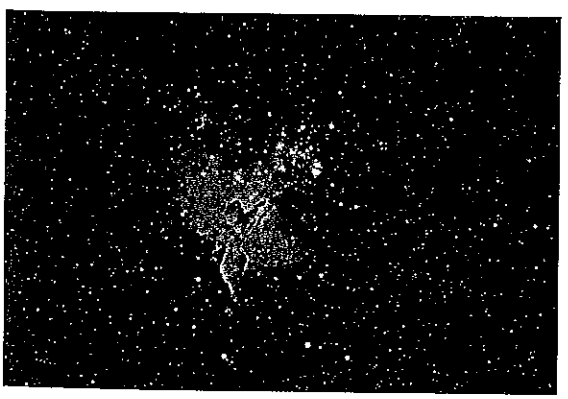

(c)

Fig. 15.6 HII regions. (a) The Lagoon Nebula (M8), in Sagittarius, at a distance of 2 kpc. It is 20 pc across. Notice the cluster of bright blue-white stars, which produce ionizing radiation. The ionized gas glows red. The name comes from the dust lane that cuts across the front, blocking our view of the gas behind. (b) HST image view of M8. (c) The Eagle Nebula (M16), in Serpens. (d) HST image of the dust lanes in M16. The bright edges are regions of recent ionization. (e) HST image of the Omega Nebula (M17), in Sgr, at a distance of 2 kpc. Here the ionizing stars are not as obvious, and are embedded deep within the nebula.

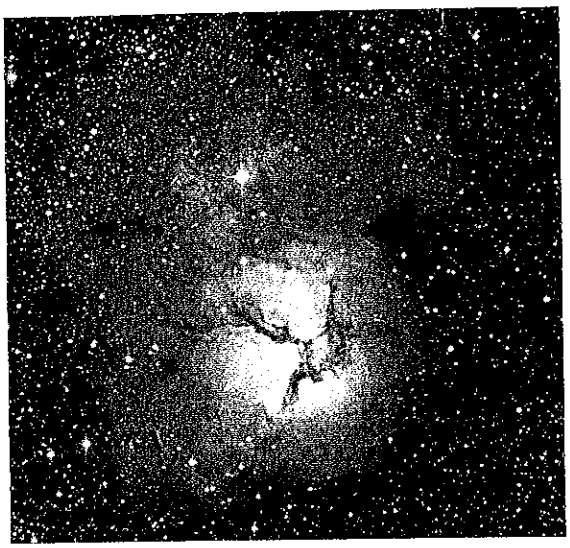

(f)

(h)

(g)

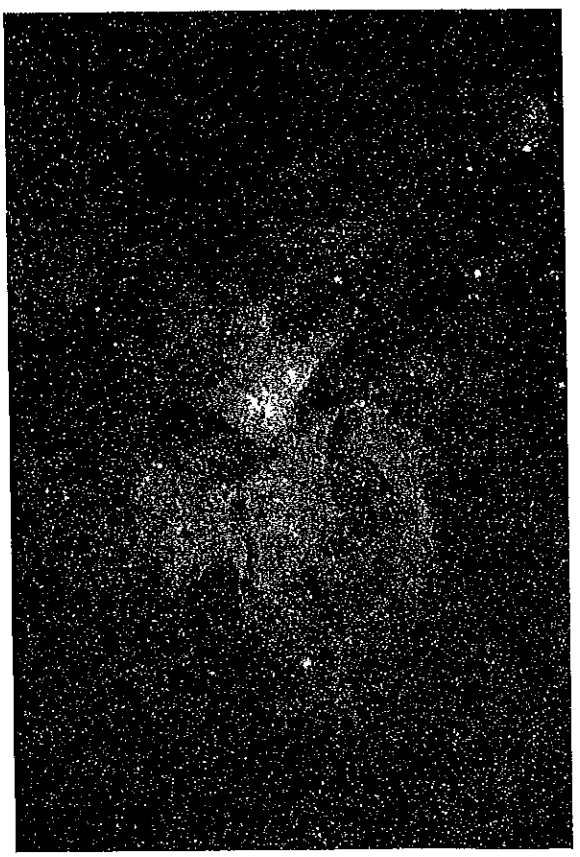

(i)

Fig. 15c (*Continued*) (f) The Trifid Nebula (M20), in Sgr. It is named for the three-part appearance produced by the dust lanes. The blue part on top is starlight reflected from associated dust, a reflection nebula. (g) HST image of M20 (h) The Rosette Nebula (NGC 2244) in Monoceros, named for its red color and petal-like appearance. The cluster of blue stars in the center has created a cavity in the center of the cloud. It is 1.3 kpc away and 15 pc across. (i) The Eta Carina Nebula (NGC 3372), named for the bright star that illuminates it. It is 3 kpc from Earth.

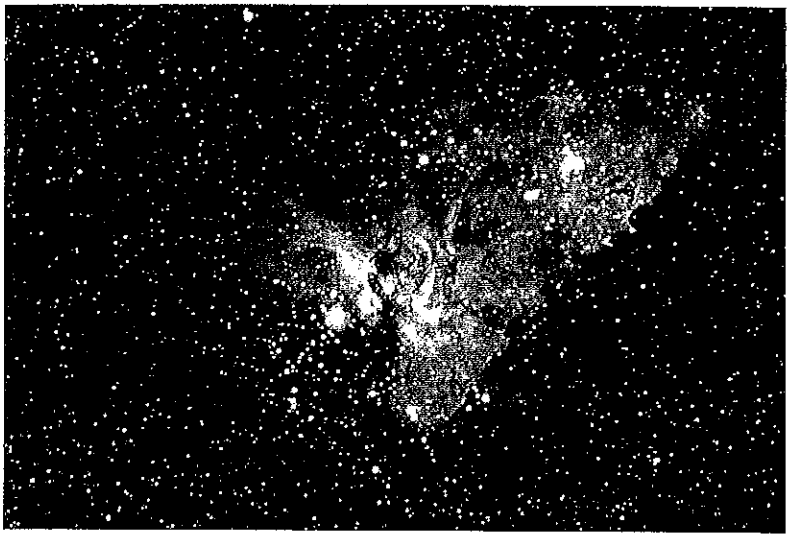

(j)

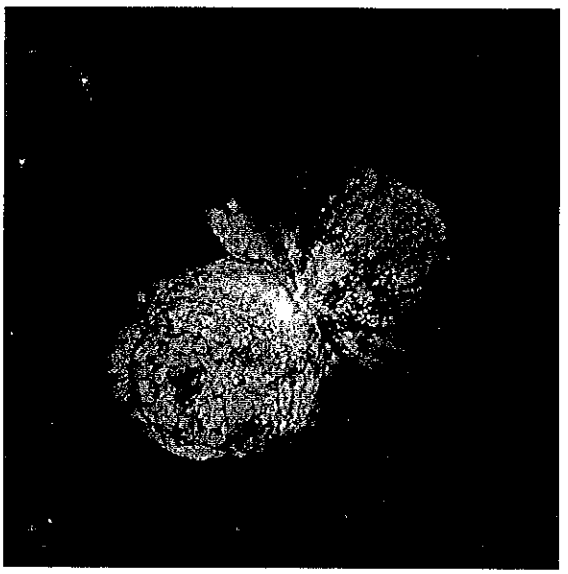

(k)

FIG 15.8 (*Continued*) (j) The central region of the Eta Carina Nebula. (k) HST image of the immediate vicinity of Eta Carina. [(a), (c), (f), (h)–(j) NOAO/AURA/NSF; (b), (d), (g), (k) STScI/NASA; (e) ESO]

Free electrons and protons collide, forming neutral hydrogen atoms. However, the ultraviolet photons from the star are continuously breaking up those atoms to form proton–electron pairs. The balance between these two processes determines how large a particular HII region can be. Within the HII region, almost all of the hydrogen is ionized. There is a rapid transition at the edge, from almost entirely ionized gas to almost entirely neutral gas. The theoretical reasons for this sharp transition were first demonstrated by the Swedish astrophysicist, *Bengt Stromgren*. For this reason, HII regions are often referred to as *Stromgren spheres*, and the radius of an HII region is called the *Stromgren radius*, r_S.

We can see how the balance between ionizations and recombinations determines the Stromgren radius. If N_{uv} is the number of ultraviolet photons per second given off by the star capable of ionizing hydrogen, then this is the number of hydrogen atoms per second that can be ionized. That is, the rate of ionizations R_i is given by

$$R_i = N_{uv} \tag{15.23}$$

The higher the density of protons and electrons, the greater the rate of recombinations. The recombination rate is given by

$$R_r = \alpha n_e n_p V \tag{15.24}$$

where V is the volume of the HII region and α is a coefficient (which depends on temperature in a known way). For the volume, we can substitute the volume of a sphere with radius r_S. If the only ionization is of hydrogen, the number density of electrons must equal that of protons, since both come from ionizations of hydrogen. Equation (15.24) then becomes

$$R_r = \alpha n_p^2 (4\pi r_S^3/3) \tag{15.25}$$

Equating the ionization and recombination rates gives

$$N_{uv} = \alpha n_p^2 (4\pi r_S^3/3) \tag{15.26}$$

Solving for r_S gives

$$r_S = (3/4\pi\alpha)^{1/3} (N_{uv})^{1/3} n_p^{-2/3} \quad (15.27)$$

From equation (15.27) we can see that the size of an HII region depends on the rate at which the star gives off ionizing photons and the density of the gas. If the gas density is high, the ionizing photons do not get very far before reaching their quota of atoms that can be ionized. The rate at which hydrogen ionizing photons are given off changes very rapidly with spectral type, as indicated in Table 15.2, so the HII region around an O7 star is very different from that around a B0 star. Often, O and early B stars are found in very small groupings. In these groupings, the HII regions from various stars overlap, and the region appear as one large HII region.

The ultraviolet radiation from stars can also ionize other elements. For example, after hydrogen, the next most abundant element is helium. However, the ionization energy of helium is so large that only the hottest stars produce significant numbers of photons capable of ionizing helium. On the other hand, the ionization energy of carbon (for removing one electron) is less than that of hydrogen. There are many photons that are capable of ionizing carbon that will not ionize hydrogen. This, combined with the lower abundance of C relative to H, means that CII regions are generally much larger than HII regions (see Problem 15.20).

There are actually two conditions under which the boundary for an HII region can exist. One is that which we have already discussed. The cloud continues beyond the range of the hydrogen-ionizing photons. When this happens, we say that the HII region is *ionization bounded*. The other possibility is that the cloud itself comes to an end while there is still hydrogen-ionizing radiation. In this case, we say that the HII region is *density bounded*, since its boundary is determined by the place where the density is so low that we no longer think of the cloud as existing. When an HII region is density bounded, hydrogen-ionizing radiation can slip out into the general interstellar radiation field. This is an important source of ionizing radiation in the general interstellar medium (i.e. not near HII regions).

The temperature of HII regions is quite high – about 10^4 K. HII regions are heated by the ionization of hydrogen. When an ultraviolet photon causes an ionization, some of the photon's energy shows up as the kinetic energy of the free proton and electron. Cooling in an HII region is inefficient, since there are no hydrogen atoms and no molecules. Cooling can only take place through trace constituents, such as oxygen. Transitions within these constituents are excited by collisions with protons and electrons. The collisions transfer kinetic energy from the gas to the internal energy of the oxygen. The oxygen then radiates that energy away. Since the heating is efficient and the cooling is inefficient, the temperature is high.

Table 15.2. | Rates of H-ionizing photons for main sequence stars.

Spectral type	Photons/s ($\times 10^{48}$)
O5	51
O6	17.4
O7	7.2
O8	3.9
O9	2.1
B0	0.43
B1	0.0033

HII regions can give off continuous radiation, which can be detected in the radio part of the spectrum. This radiation results from collisions between electrons and protons in which the two do not recombine. Instead, the electron scatters off the proton. In the process the electron changes its velocity. When a charged particle changes it velocity, it can emit or absorb a photon. This radiation is called *Bremsstrahlung* (from the German for "stopping radiation"). It is also called *free–free radiation*, because the electron is free (not bound to the proton) both before and after the collision. The spectrum of free–free radiation (Fig. 15.9) is characterized by the temperature of a gas. The spectrum is not that of a blackbody because the gas is not optically thick. The spectrum is a blackbody curve multiplied by a frequency dependent opacity. Because the radiation can be described by the gas temperature, it is also known as *thermal radiation*. This radiation is strongest in the radio part of the spectrum. Therefore, we can use radio continuum observations to see HII regions anywhere in our

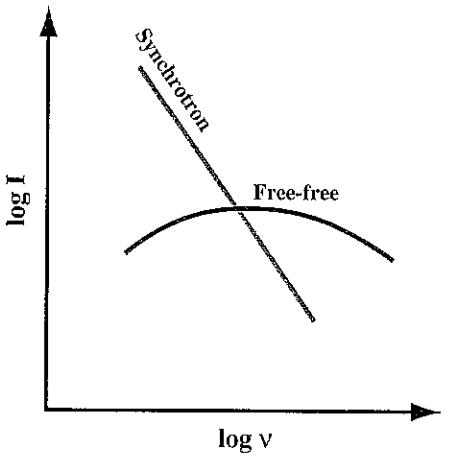

Fig. 15.9 Schematic spectra of synchrotron radiation and free–free emission. The vertical axis is intensity and the horizontal axis is frequency, both on a logarithmic scale. The log–log representation emphasizes the power-law behavior of the synchrotron radiation

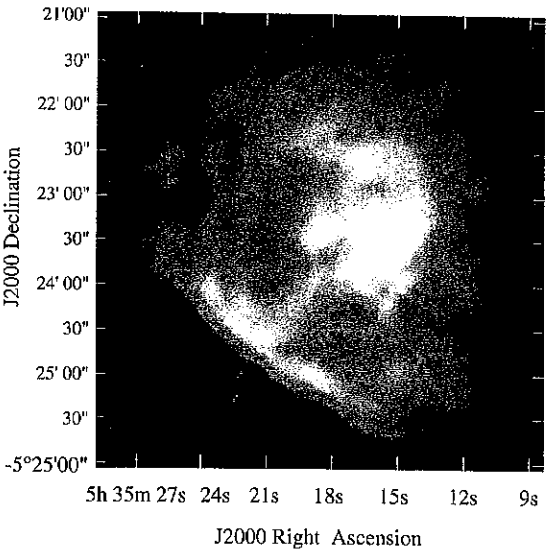

Fig. 15.10 Radio image (made with the VLA) of free–free emission from an HII region, the Orion Nebula (for which optical images appear in Fig. 15.28). This is a higher resolution image than the single dish version in Fig. 4.25. It shows the fine scale structure in the core of the nebula. The image was made with the VLA in D (smallest) configuration at 8.4 GHz, providing 8.4 arc sec resolution. This is a nine-field (3 × 3) mosaic. The interferometer picks up less than one-half of the total flux density because it is insensitive to the extended emission. Of course, it also gives beautiful detail of the structure in the nebula. [D. Shephard, R. Maddalena, J. McMullin, NRAO/AUI/NSF]

galaxy. A map of continuum emission from an HII region is shown in Fig. 15.10. (Note: In the encounter between the electron and proton, the proton also accelerates and gives off radiation. However, the acceleration of the proton is much less than that of the electron, by the ratio of their masses. This means that the radiation given off by the protons is not very important.)

HII regions also give off spectral line radiation, called *recombination line* radiation. When an electron and proton recombine to form a hydrogen atom, the electron often ends up in a very high state. The electron then starts to drop down. It usually falls one level at a time. Larger jumps are also possible, but less frequent. With each jump, a photon is emitted at a frequency corresponding to the energy difference for the particular jump. (The energies are given by equation 3.6.) For very high states, the energy levels are close together and the radiation is in the radio part of the spectrum. As the electron jumps to lower states the lines pass through the infrared and into the visible. Generally, the electron can go all the way down to the ground state before the atom is re-ionized. We even see Hα emission as part of this recombination line series. This gives HII regions a red glow. (This red glow allows us to distinguish HII regions from reflection nebulae, which appear blue.)

HII regions expand with time. When an HII region first forms (Fig. 15.11), it must grow to its equilibrium radius. Even after it reaches this equilibrium size, it will continue to expand. This is because the pressure in the HII region is greater than that in the expanding cloud. The higher pressure results from the higher temperature in the HII region. Remember, the temperature in an HII region is about 10^4 K, while that in the surrounding cloud is less than 100 K. The densities in the HII region and surrounding cloud are similar.

As the HII region expands, it can compress the material in the surrounding cloud, possibly initiating a new wave of star formation, as illustrated in Fig. 15.12. This is one possibility that has been discussed for the triggering of star formation. The gas compressed by an expanding HII region will not automatically form stars. That is because the gas will be heated as it is compressed. If that heat is not lost, the temperature of the cloud will increase.

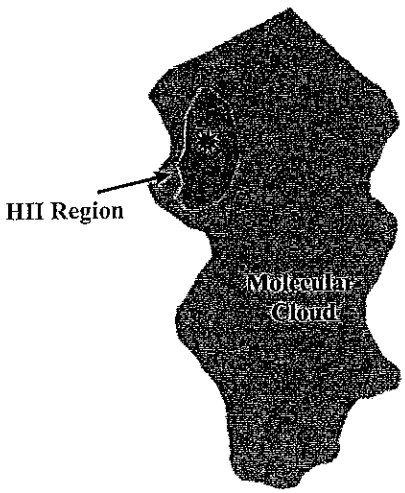

Fig. 15.11 HII region in a molecular cloud. HII regions usually form near the edge.

The pressure will increase and the gas will expand again. The re-expansion of compressed gas can only be avoided if the gas can cool as it is compressed. Radiation from molecules such as CO in the surrounding cloud can help with this cooling process.

15.6.2 Masers

We have already seen how the process of stimulated emission can lead to a multiplication – or amplification – in the number of photons passing through a material. In the stimulated emission process, one photon strikes an atom or molecule, and two photons emerge. The two photons are in phase and are traveling in the same direction. The fact that they are in phase means that their intensities add constructively. Stimulated emission can only take place if the incoming photon has an energy corresponding to the difference between two levels in the atom or molecule, and the atom or molecule is in the upper of the two levels.

If only a few atoms or molecules are in the correct state, there will not be a significant increase in the number of photons. Suppose we designate the two states in the transition as 1 and 2. The population of the lower state is n_1 and the population of the upper state is n_2. The requirement for amplification is that n_2/n_1 be greater than g_2/g_1, where the g are the statistical weights. The situation is called a *population inversion*, since it is the opposite to the normal situation. Formally, it corresponds to a negative temperature in the Boltzmann equation (see Problem 15.22). This is clearly not an equilibrium situation. The population inversion in a particular pair of levels must be produced by a process, called a *pump*. The pump may involve both radiation and collisions. The net effect of the pump process is to put energy into the collection of atoms or molecules so that some of that energy can come out in the form of an intense, monochromatic, coherent (in phase) beam of radiation.

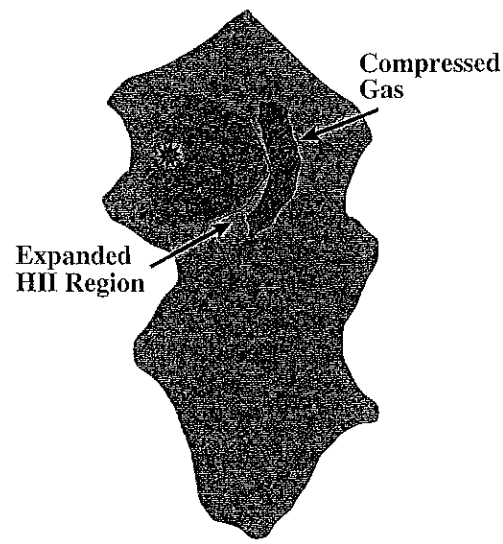

Fig. 15.12 The HII region expands, compressing gas deeper within the cloud. If this gas can cool quickly, then it can collapse to form more stars.

This was first realized in the laboratory, in the 1950s, by *Charles Townes* (then at Columbia University). Townes won the Nobel Prize in physics for this work. Since microwaves were being amplified in the process, the device was called a *maser* (Fig. 15.13), an acronym for *m*icrowave *a*mplification by *s*timulated *e*mission of *r*adiation. Subsequently, *lasers* were developed for the amplification of visible light. In any laser or maser, two things are necessary: (1) a pump to provide the population inversion, and (2) sufficient path length to provide significant amplification. In interstellar space, the path length is provided by the large side of interstellar clouds. In the laboratory that path length is provided by mirrors. (Laboratory masers are used as amplifiers in some radio telescope receivers.)

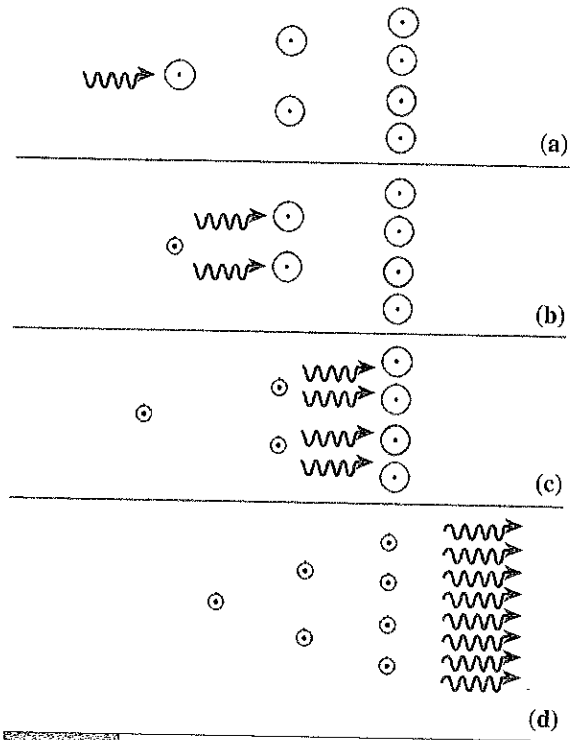

Fig. 15.13 Maser amplification. In each frame, a molecule in the upper level of the maser transition is indicated by a large circle, and one in the lower level is indicated by a small circle. (a) All of the molecules are in the upper state, and a photon is incident from the left. (b) The photon stimulates emission from the first molecule, so there are now two photons, in phase. (c) These photons stimulate emission from the next two molecules, resulting in four photons. (d) The process continues with another doubling in the number of photons.

Shortly after the development of laboratory masers, an interstellar maser was discovered. It involved the molecule OH. Four emission lines of OH were observed, but their relative intensities were wrong for a molecule in equilibrium. As radio telescopes were developed with better angular resolution, the emission was observed to become stronger and stronger. This means that the emission is probably very intense, but coming from a very small area. This behavior was suggestive of an interstellar maser. The next maser discovered was in the water (H_2O) molecule, at a wavelength of 1 cm. As observations with better resolution became possible, it was clear that the objects were giving off as much energy as a 10^{15} K blackbody over that narrow wavelength range in which the emission was taking place.

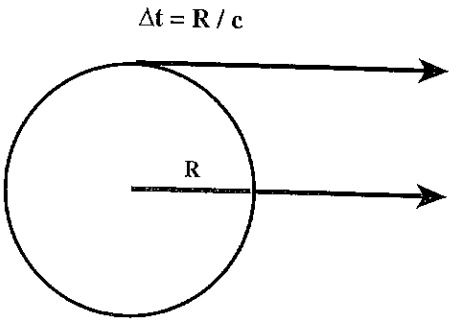

Fig. 15.14 Time variability and source size. The signal from the farthest point the eye can see must travel an extra distance R over that from the nearest point the eye can see.

A small size for these sources was also deduced from rapid variations in their intensity. Suppose we have a sphere of radius R, as shown in Fig. 15.14. If the sphere were suddenly to become luminous, then the first photons to leave each point on the surface would not reach us simultaneously. The photons from the edge of the sphere have to travel a distance R farther than the photons from the nearest point. These photons will arrive a time $\Delta t = R/c$ later than the first photons. Therefore, it will take this time for the light we see to rise from its initial low level to the final high value. A similar analysis holds for the time it would take for us to see the light turning off.

The above analysis tells us that an object's brightness cannot vary on a time scale faster than the size of the emitting region, divided by c. If we see variations in intensity over a time scale of a year, the source cannot be larger than a light year across. Interstellar masers were found to vary in intensity on an even shorter time scale, of the order of a month, indicating an even smaller size.

Example 15.7 Maser size

Estimate the maximum size of a maser that varies on the time scale of one month. What is the angular size of this object at a distance of 500 pc?

SOLUTION

The time scale for the variations is

$$\Delta t = (24 \text{ h/day})(3600 \text{ s/h})(30 \text{ day})$$
$$= 2.6 \times 10^6 \text{ s}$$

This corresponds to a size of

$$R = c\Delta t$$

$$= 7.8 \times 10^{16} \text{ cm}$$

$$= 5.2 \times 10^{3} \text{ AU}$$

The angular size (in arc seconds) is related to R (in AU), and the distance d (in pc) by (equation 2.16)

$$\theta(") = R(\text{AU})/d(\text{pc})$$

$$= 5.2 \times 10^{3} / 500$$

$$= 10 \text{ arc sec}$$

In fact, masers are even smaller than this size, and have angular extents much less than 1 arc second. This means that we need radio interferometers to study masers. Very long baseline interferometry has been used to study masers.

When we try to understand interstellar masers we must explain both the pump and the path length for the gain. Many of the theories require very high densities. For example, we think that the presence of water masers suggests densities in excess of 10^8 cm^{-3}. This is much denser than even the dense cores that we normally see in molecular clouds. We therefore think that masers are associated with objects collapsing to become protostars. We take the presence of H_2O or OH masers in a region to indicate the possibility of ongoing star formation.

When we observe masers, we often see them in clusters, such as that depicted in Fig. 15.15. With radio interferometry, we can measure the positions of the masers very accurately. We can even measure their proper motions. We can use Doppler shifts to measure their radial velocities. However, we expect the motions of a cluster to be random, so the average radial velocity should equal the average transverse velocity v_T. From equation (13.6) we see that the distance is related to the proper motion and transverse velocity by

$$d(\text{pc}) = v_T(\text{km/s})/4.74\mu(\text{arc sec/yr})$$

Therefore, an accurate study of the motions of masers allows us to determine the distance to a cluster of masers. It is hoped that this will develop into a very powerful distance measuring technique. This technique works equally well for random motions or for the masers being in an expanding shell. The only requirement is that the average velocity along the line of sight is the same as the average velocity perpendicular to the line of sight.

Maser emission is also observed in the molecule SiO (silicon monoxide). From the regions in which it is observed, it seems that SiO maser emission is associated with mass outflow from evolved red giant stars. Also, some OH masers are associated with similar regions.

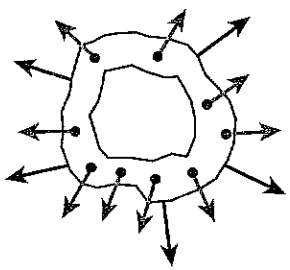

Fig. 15.15 Cluster of masers in an expanding shell.

15.6.3 Energetic Flows

A major recent discovery is that many regions of star formation seem to be characterized by strong outflows of material. One piece of evidence for such flows comes from the observation of very broad wings on the emission lines of CO (Fig. 15.16). The widths of these wings range from 10 to 200 km/s. The broad wings are usually seen only over a small region where the CO emission is strongest. A peculiar feature of this emission is that the redshifted wing and blueshifted wing seem to be

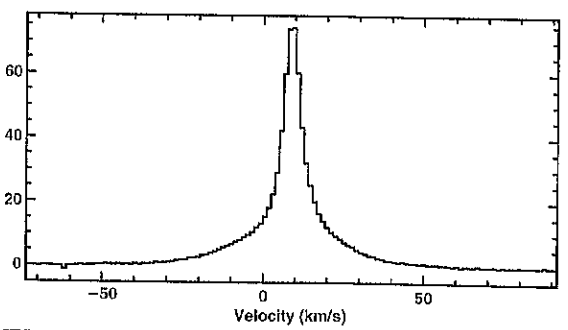

Fig. 15.16 Spectrum of the 2.6 mm CO emission line from the core of the molecular cloud behind the Orion Nebula (Fig. 15.28.) The broad wings extend many tens of kilometers per second on both sides of the line center. [Jeffrey Mangum, NRAO/AUI/NSF]

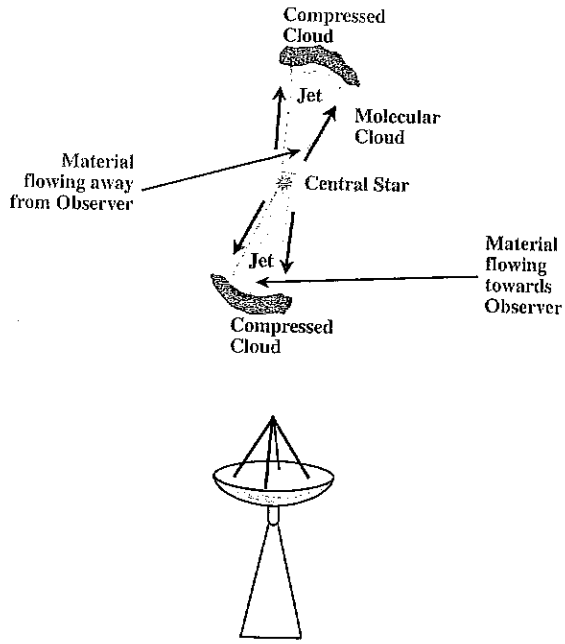

Fig. 15.17 Model for a bipolar flow. Material coming towards us on the near side of the cloud is blueshifted. Material going away from us on the far side of the cloud is redshifted. If the flow is not aligned along the line of sight, the redshifted and blueshifted emission will appear in different locations on the sky.

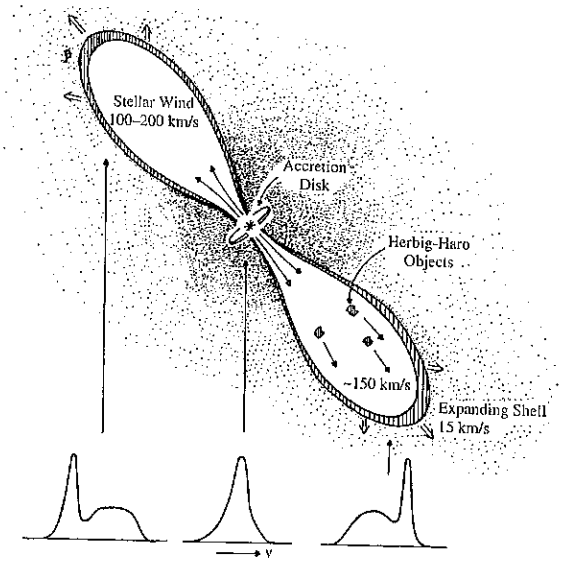

Fig. 15.18 A model for sources with bipolar flows and HH objects. The stellar wind comes out in all directions but is blocked in most directions by a disk around the star. The wind emerges mostly at the poles of the disk. This drives material in the surrounding cloud away. Below, the effects of the motion on the CO line profiles are shown, assuming that the wind to the upper left moves away from the observer and the wind to the lower right moves towards the observer. [Ronald Snell (University of Massachusetts) Snell, R. A. *et al.*, *Astrophys. J. Lett.*, **239**, L17, 1980, Figs. 2 & 5]

coming from different parts of the cloud. This suggests that we are seeing two jets of gas, one coming partially towards us and the other partially away from us, as shown in Fig. 15.17. Because of this structure, we call these objects sources of *bipolar flows*.

Actually, we could also envision a model in which we are seeing infall rather than outflow. However, there is evidence we are seeing the effects of a wind striking the surrounding cloud, heating a small region. These small heated regions show emission in the infrared from H_2, requiring temperatures of about 10^3 K. Current theories of these sources involve strong stellar winds, as shown in Fig. 15.18. The star is also surrounded by a dense disk of material. This disk blocks the wind in most directions, but allows it to escape along the axis, explaining the bipolar appearance. Remember, we saw earlier in this chapter that disks are likely to form around the collapsing star.

Evidence for collimated winds is present in another interesting class of objects that we think are associated with pre-main sequence stars, the *Herbig–Haro (HH) objects* shown in Fig. 15.19; see also Fig. 15.20. They were discovered independently by *George Herbig* of the Lick Observatory and *Guillermo Haro* of the Mexican National Observatory. HH objects appear as bright nebulosity on optical photographs. Their spectra resemble those of stars, and usually show emission lines, but no star is present in the nebulosity (Fig. 15.21). We now think that the wind from a pre-main sequence star clears a path through the cloud. The part of the cloud where the wind runs into the cloud is heated, and glows. We also see starlight reflected from the dust, explaining the stellar spectrum. The exciting star is deep within the cloud and is not seen directly.

These observations indicate that winds are an important feature of protostellar evolution for most stars. For low mass stars such as the Sun,

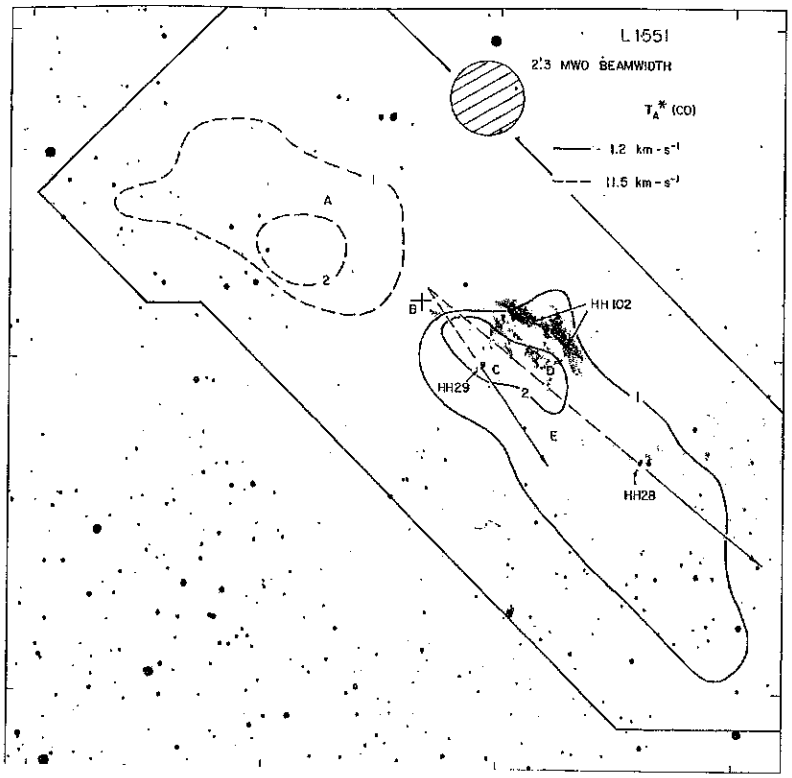

Fig. 15.19 A negative optical image of a region, containing a bipolar flow and a number of Herbig–Haro objects. The solid contours are the CO emission that is blueshifted with respect to the average velocity. The dashed contours show the redshifted CO. The plus (+) marked B is the location of the suspected source for the flow. [Snell, R. A. *et al., Astrophys. J. Lett.*, **239**, L17, Figs. 2 & 5]

this wind is relatively gentle, and can clear some of the debris from around the forming star, leaving any planetary system intact. For massive (O and B) stars the strong winds drive away a large mass. It has been suggested that the combined effects of winds in OB associations can drive off enough mass to unbind the association, explaining why associations are not gravitationally bound. Winds can also carry away some of the angular momentum in a cloud, allowing the collapse of the remaining material to continue.

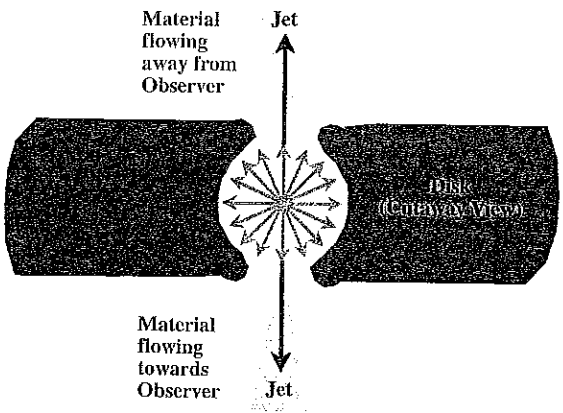

Fig. 15.20 How an isotropic flow can be converted into two jets. The source of the isotropic outflow is in a hole in a disk. In most directions the disk can block the flow, but not in the direction where the disk is thinnest. Jets emerge in that direction.

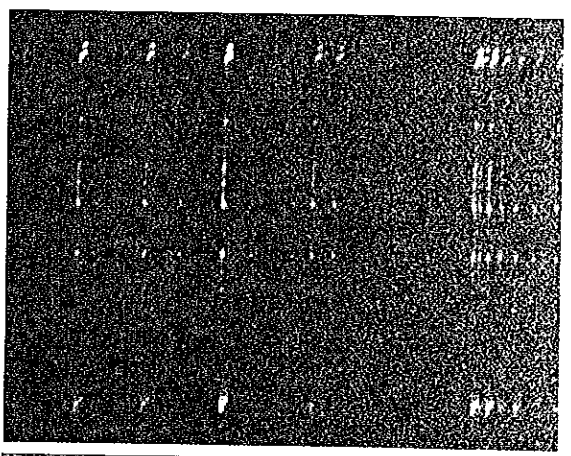

Fig. 15.21 IR spectrum of Herbig–Haro object number 212. Notice the bright emission lines. [ESO]

(a)

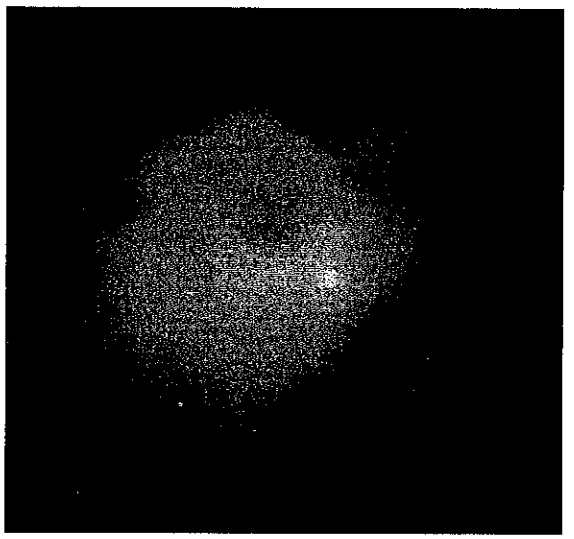

(b)

Fig. 15.22 Images of two T Tauri stars. (a) T Tauri. The star is unremarkable, but there is a small nebula to the right. The star is in a dust cloud. The presence of the dust can be deduced from the fact that it blocks light from the background stars. There are therefore fewer background stars in the center of the photograph than around the edges. (b) HL Tau. Again, there is some nebulosity near the star and the star is in a dust cloud. [(a) Courtesy of 2MASS/UMASS/IPAC/NASA/JPL/Caltech; (b) Laird Close, (University of Arizona)/Close, L., *Astrophys. J.*, **486**, 766, 1997]

15.6.4 T Tauri stars and related objects

Another group of pre-main sequence objects are called *T Tauri stars* (Fig. 15.22). T Tauri is a variable star in the constellation Taurus, and T Tauri stars are variables with properties like those of T Tauri. Light curves are shown in Fig. 15.23, and a spectrum is shown in Fig. 15.24. These stars are spectral class K, and appear above the main sequence on the HR diagram. These show an irregular variability. Their spectra are also characterized by the presence of emission lines.

There are three possible sources of the variability we see:

(1) The variability could arise in a photosphere. One model for this involves star spots. These are dark areas, like sunspots, only larger. As the star rotates, a different fraction of the

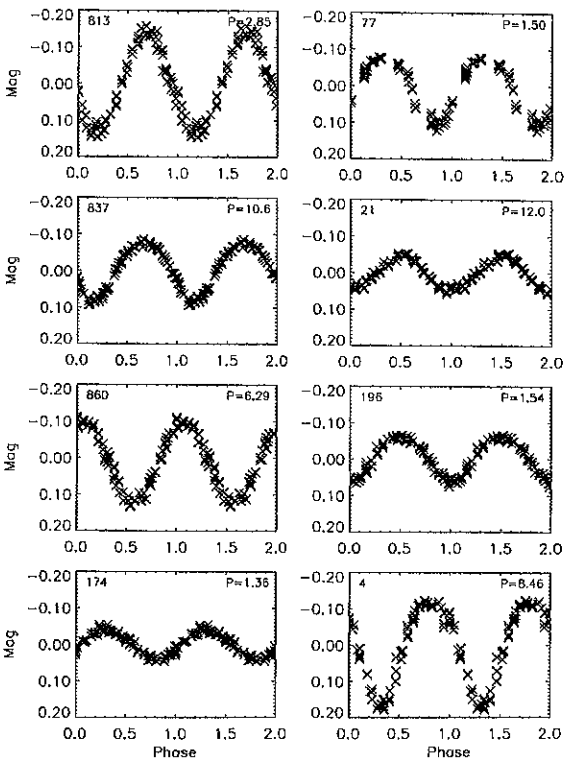

Fig. 15.23 Light curves for a selection of T Tauri stars in the Orion Nebula cluster. The horizontal axis is fractions of a period (which is given in days in the upper right-hand corner of each curve). Variability is caused by rotation of stars with large, cool spots. [William Herbst (Wesleyan University)/Herbst, W. *et al.*, *Astrophys. J. Lett*, **554**, L197, 2001]

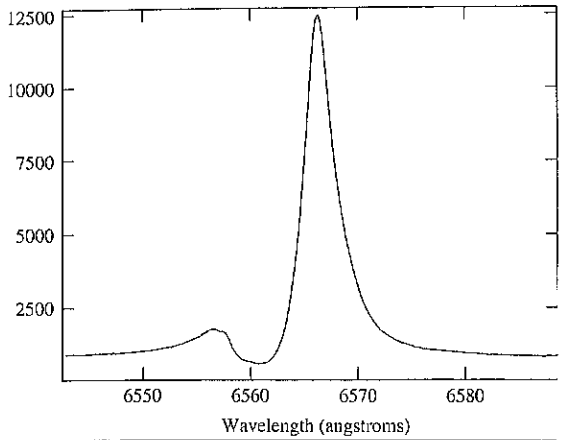

Fig. 15.24 Strong Hα emission line from a T Tauri star. [George Herbig, IFA, Hawaii]

observed surface is covered by the spots, and the brightness changes.

(2) The variations may arise in the chromosphere.

(3) The variations may actually result from changes in the opacity of the dust shell surrounding the star.

The emission lines show Doppler-shifted absorption wings, like those in Fig. 15.24. This suggests material both falling into the star and material coming off the star. The infall may be close to the star as the final stage of collapse, while the outflow is a wind (like the solar wind, but stronger) farther away from the star. Alternatively, the infall may be in the form of a disk around the star's equator, while the outflow is along the polar axes.

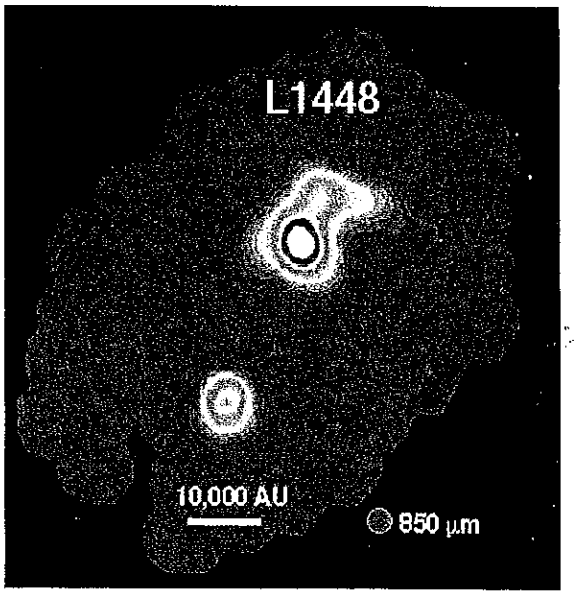

Fig. 15.25 Far IR image of protostellar core. This is a ground-based image from Mauna Kea, at 850 μm. The beam size is shown in the red circle to the lower right, so you can see that the sources are barely resolved. Notice the separation into two sources. The irregular edges of the image are due to problems with the detectors near the edge. This is an example of what is called a Class 0 protostar, which is thought to be the youngest stage, where there is a strong outflow but the surrounding cloud has not been driven away. [Yancy Shirley, University of Texas, Austin, made with SCUBA on the JCMT]

From studies of the spectral lines, we think that the winds may have speeds of about 200 km/s. The mass loss in the wind, dM/dt, is about 10^{-7} $M_\odot$/yr. The total luminosity in the

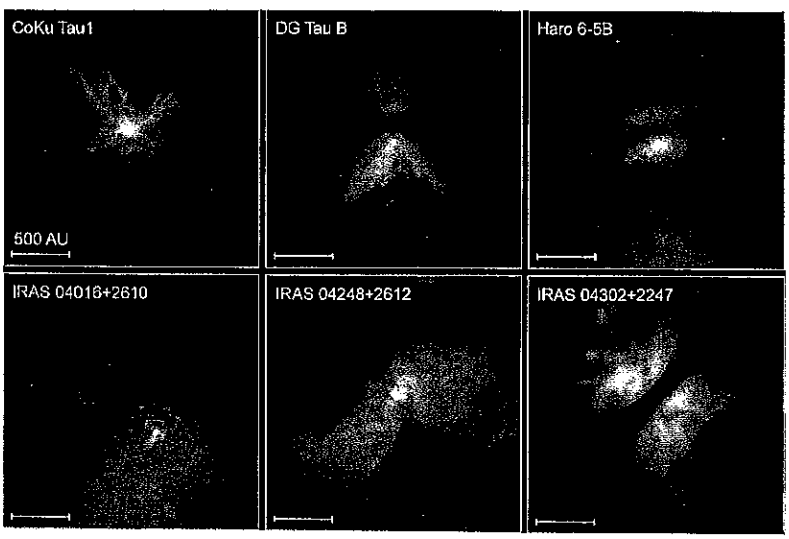

Fig. 15.26 HST images of infrared emission from selected disks around forming stars. All six objects are in Taurus, at a distance of 150 pc. [STScI/NASA]

wind is that rate at which kinetic energy is carried away in the wind,

$$L_w = (1/2)(dM/dt)v^2 \quad (15.28)$$

Using the numbers given, we find a wind luminosity of about 1 $L_\odot$. That is, the star gives off as much energy per second in its wind as the Sun gives off at all wavelengths. However, the wind phase is a short lived one. The wind does sweep away some of the dust that has collected around the star. We think that a similar wind from the Sun was important in clearing debris out of the early Solar System.

It is now possible to make far IR images of protostellar cores, like that in Fig. 15.25. Far IR emission HST and IR satellites have provided us with some images, such as those in Fig. 15.26, which may be the result of infrared emission from dust shells around recently formed stars. Molecular spectral line observations of these disks will require resolutions achievable using interferometers.

15.7 Picture of a star forming region: Orion

The Orion region (Fig. 15.27) is one of the most extensively studied star forming regions. It is relatively nearby, only about 500 pc from the Sun. It is away from the plane of the Milky Way, so there is little confusion with foreground and background stars. There is also an interesting variety of activity in this region.

The region contains a large OB association. There are four distinct subgroups. The two oldest are near Orion's belt, and the two youngest are near the Orion Nebula (Fig. 15.28a) in Orion's sword. The Orion Nebula is an HII region powered by the brightest stars in the youngest subgroup. Images of the Orion Nebula and its cluster are in Figs. 15.28(b)–(e).

The region also contains two giant molecular cloud complexes, also shown in Fig. 15.4. A far IR image of the GMCs is shown in Fig. 15.27(a). The northern complex is associated with the belt region, which contains the two oldest subgroups, and a strong HII region just north of the Horsehead Nebula. The southern complex is associated with the sword region, which contains the two youngest subgroups. The southern complex contains the Orion Nebula and several smaller HII regions. The Orion Nebula is actually on the front side of the molecular cloud. Behind the HII region is a dense molecular core. It is totally invisible in the optical part of the spectrum because of the foreground material. However, it can be studied in detail using radio observations of molecules. In addition, it is a source of infrared emission.

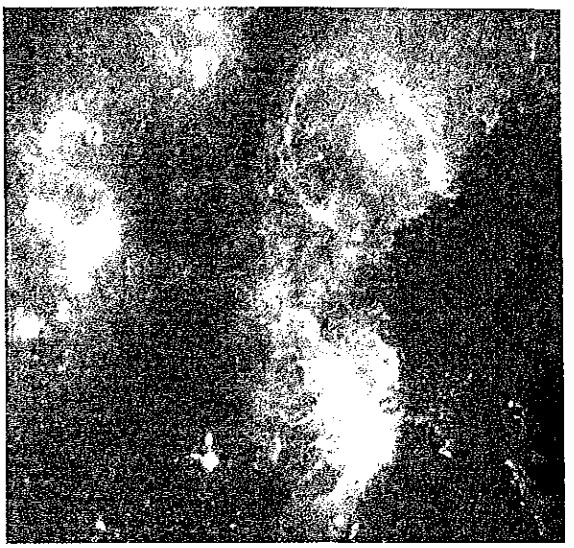

(a)

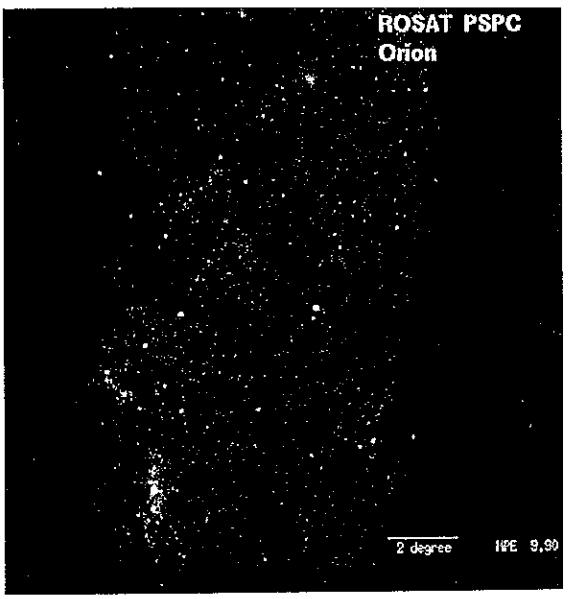

(b)

Fig. 15.27 Large-scale images of the Orion region, mostly at a distance of 500 pc. (a) Far IR image from IRAS. (b) X-ray image from ROSAT. [(a) NASA, (b) NASA/MPI]

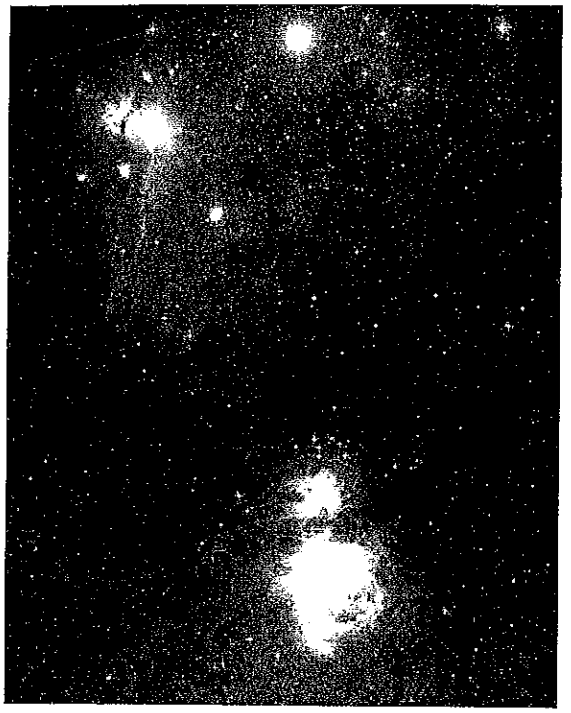

(a)

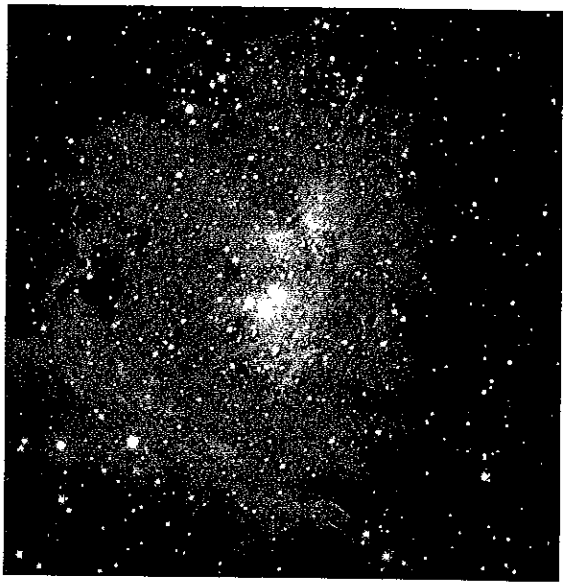

(c)

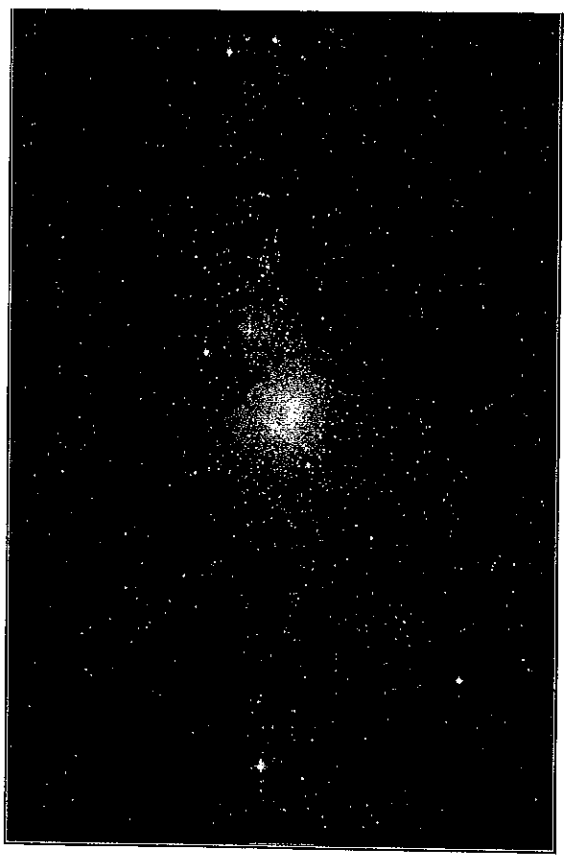

(b)

(d)

Fig 15.28 Images of the Orion region, mostly at a distance of 500 pc. (a) Large scale view of the belt and sword regions. Two of the three belt stars appear at the top of the image. The lower left belt star illuminates an HII region that has the Horsehead Nebula superimposed. The sword region is near the bottom. The Orion Nebula is overexposed in this image, and surrounds the central sword star. (b) The Orion Nebula. There is a small cluster of O and B stars that ionize this nebula. A dense dust cloud provides over 100 mag of visual extinction in the central part. The object near the top of the photo is a separate small HII region illuminated by a single star. Compare its simple appearance to the complex structure of the big nebula.

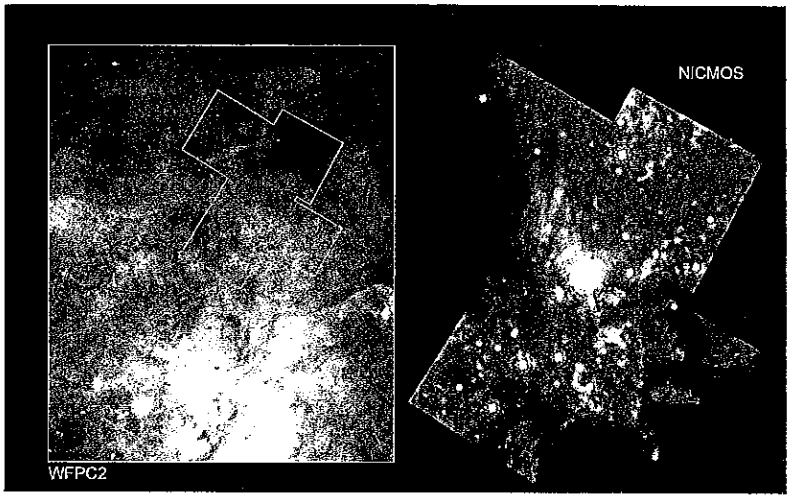

(e)

FIGURE 15-28 (*Continued*) (c) Central part of the Orion Nebula. This gives a better view of the O and B stars. The brightest four stars in the central part of the cloud are called the Trapezium, because of their arrangement. Notice the dense dark cloud intruding from the upper left. (d) A larger field HST image of the Orion Nebula, assembled from 15 smaller field images. This image is approximately 1 pc across. (e) HST image of filaments in the nebula. The diagonal length of this image is 0.5 pc. The plume of gas at the lower left is the result of a wind from a newly formed star. Red light depicts emission in nitrogen; green is hydrogen; blue is oxygen. [(a) © Anglo-Australian Observatory/Royal Observator, Edinburgh. Photograph from ULK Schmidt plates by David Malin; (b) Courtesy of 2MASS/UMASS/IPAC/NASA/JPL/Caltech; (c) ESO; (d), (e) STScI/NASA]

The general picture of the southern complex that has emerged has the HII region expanding into the molecular cloud, compressing it. This compression probably triggered a new generation of star formation. This new cluster of stars now appears as a series of small infrared sources and masers. There is evidence for an energetic flow. We see very broad (over 100 km/s) lines in CO and other molecules. These wings have the characteristics of the bipolar flows discussed in the preceding section. We also see evidence for small regions of gas heated to high temperatures in the regions where the wind strikes the surrounding cloud. Infrared line emission from H_2 is seen from this 2000 K gas. We can also study the proper motions of the maser and see that the region is expanding. (The best measurement of the distances to this region comes from studying the proper motions of masers, as discussed in the preceding section.) It is likely that this dense region will appear as another OB subgroup when there has been sufficient time to clear the interstellar material away.

Chapter summary

In this chapter we saw how the various components of the interstellar medium, discussed in Chapter 14, are involved in the process of star formation. We first looked at the conditions for gravitational binding, and found that molecular clouds are the likely sites of star formation. Current problems in star formation include how the collapse is actually initiated, what fraction of the mass is converted into stars, how planetary systems form, and how OB associations form. We saw how rotation can slow or stop the collapse, and lead to the formation of binaries, planetary systems and disks.

We saw how the magnetic field in a cloud can affect its collapse if the magnetic energy is comparable to the gravitational potential energy. As a cloud collapses, we expect that flux freezing will lead to an increase in the magnetic field strength within the cloud. We saw that there are two ways to overcome the support the

magnetic field provides. One produces a stead stream of low mass stars, and the other pr duces waves of high mass (as well as low mas star formation.

We saw how the molecular clouds, being cool and dense, are the most likely sites of star formation. The most massive stars seem to be born in the giant molecular clouds. These clouds have masses in excess of $10^5\ M_\odot$ and are found in complexes with masses in excess of $10^6\ M_\odot$.

We looked at how collapsing clouds eventually become protostars, glowing mostly in the near infrared. Their radiation is provided by the decrease in the gravitational potential energy as the cloud collapses.

O or early B star forms in a molecular as around the cloud is ionized, pro- I region. The size of the HII region is by a balance between ionizations and recombinations. The continuous radiation from HII regions comes from free–free scattering of electrons. Recombinations lead to electrons passing through many energy levels, giving off recombination line radiation.

Other indicators of recent star formation are masers and energetic flows. The bipolar flows provide indirect evidence for the existence of disks that collimate the flows.

We looked at the Orion region as an nearby example of ongoing high and low mass star formation.

Questions

15.1. Explain why cool dense regions are the most likely sites of star formation.

15.2. Suppose we have a cloud of 2 pc radius, formed of a material whose Jeans length is 10 km. Will the cloud collapse?

15.3. As a cloud collapses, what happens to the Jeans mass of the new individual fragments?

15.4. If a cloud has a higher density in the center than at the edge when its collapse starts, explain what happens to the density contrast between the center and the outer part as the collapse continues. (Hint: Think about free-fall time.)

*15.5. As a cloud collapses, the acceleration of the particles increases. Therefore, the free-fall time will be less than we would calculate on the basis on constant acceleration. However, we still use the initial free-fall time as an estimate of the total free-fall time. Why does this work? (Hint: Think in terms of the time for the radius to halve, and halve again, and so on.)

15.6. Explain why a rotating cloud flattens as it collapses.

15.7. How does the formation of multiple star systems help in the star formation process?

15.8. As a cloud collapses, is it likely that it will rotate as a rigid body (ω independent of r)?

15.9. What do we mean by a "trigger" for star formation?

15.10. How is it possible for a gravitationally bound cloud to give birth to a gravitationally unbound association?

15.11. (a) What is the difference between ionization bounded and density bounded HII regions? (b) Why are density bounded HII regions important?

15.12. Explain why the CII zone around a star is much larger than the HII region. Consider (a) the relative ionization energies, and (b) the relative abundances.

15.13. Explain why almost all carbon ionizations result from photons with energies between the ionization energy of carbon and that of hydrogen, even though photons that can ionize hydrogen can also ionize carbon.

15.14. Why is the temperature of an HII region so high?

15.15. (a) How can an expanding HII region trigger star formation? (b) Why is the rate at which the gas can cool important to the process?

15.16. Why is coherence important for a maser?

15.17. How do we know that masers are small?

15.18. What features of T Tauri stars lead us to believe that they are still in the formative process?